Recent Progress in Developing a Tandem-bladed Centrifugal Compressor Stage

Ing. David Hlaváček

Thesis supervised by: doc. Ing. Daniel Hanus, CSc., EUR ING., AFAIAA

Abstract
This paper gives a summary of the last year of ongoing development of a centrifugal compressor stage with a tandem-bladed impeller for use in aircraft engines. The newly developed stage is based on a conventional stage developed at VZLÚ, a.s. from which experimental data are available, and preserves some of its geometry (the number of blades, their lean angle at the impeller exit, the outer proportions, and the shape of its meridional section). During the development of this new stage, a numerical model was made the results of which correspond closely to the experimental data. Afterwards, several variations of the tandem-bladed stage were developed. The results obtained so far indicate that there is a real possibility of improving the integral parameters of the stage (its total pressure ratio, isentropic efficiency, and mass flow parameter).

Keywords
centrifugal compressor, turboprop engine. impeller, vaned diffuser, secondary flow, CFD

1 Introduction

The centrifugal compressor stage with a tandem-bladed impeller, already presented in the last year's conference, represents an innovation in centrifugal compressor design.

The tandem-bladed stage is based on a conventional stage (further called the baseline stage), originally developed by Walter Engines, a.s. (now GE Aviation Czech) in cooperation with VZLÚ, a.s. (Aerospace Research and Test Establishment).

Fig. 1. *A study of a tandem-bladed impeller [5]*

The term tandem impeller blading means that the impeller blades are transversely divided in two parts after the inducer (see Fig. 1). The inducer part of the blades is thus made up of an axial blade vane while the exducer part consists of standard radial blading, including splitter blades. The trailing edges of the inducer blades are placed inside every second exducer passage. This arrangement positively affects the formation of boundary layers on the impeller blade surfaces. After the inducer parts of the blades, its growth is interrupted, and the resulting wake flow is directed into the middle of the downstream exducer channel. This should result in reducing the size of the wake region at the impeller exit which, in turn, leads to increasing the compressor stage isentropic efficiency.

During last year, a lot of computational time was spent proving this assumption. First, a numerical model of the baseline stage was developed and its results were compared to the experimental data. Then, after the model of the baseline stage was validated, further computations were made which already involved tandem blading. The results obtained so far show that there actually is a potential to significantly improve the integral parameters of the stage.

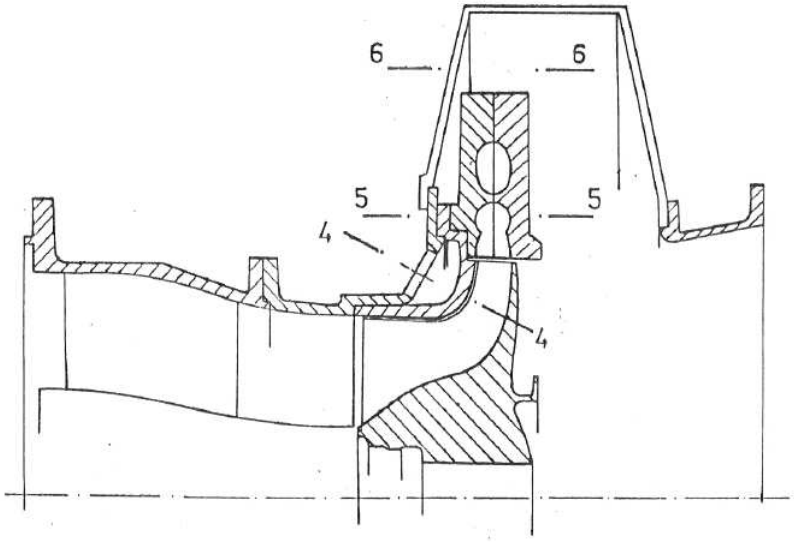

Fig. 2. *M 602 low-pressure centrifugal compressor test rig [7]*

2 Modeling the baseline compressor stage

2.1 The stage geometry

The meridional section of the baseline stage is shown in Fig. 3 There were several experimental configurations of the baseline stage to choose from. The main difference between them was the length of their splitter blades. All of these configurations were tested using a simple computational model to see the main characteristics of the flow field inside the impeller. The 410.B1 configuration (with the shortest splitter blades) was chosen because of the most advantageous flow field (see Fig. 8 and Fig. 7). The other configurations, 410.B1L and 410.B1LS, both suffered from the presence of an area of flow separation at the suction sides of the splitter blades, just downstream of their leading edges.

Tab. 1. *Baseline compressor stage design point parameters*

Parameter	**Value**
Total pressure ratio π	4.143
Mass flow rate m	7.5505 kg.s^{-1}
Mass flow parameter $Q = m\frac{\sqrt{T_{1,\,\mathrm{tot}}}}{p_{1,\,\mathrm{tot}}}$	1.3851
Isentropic efficiency η_{is}	80.8 %
Total temperature rise $\Delta T_{\mathrm{tot}} / T_{1,\,\mathrm{tot}}$	185.9 K

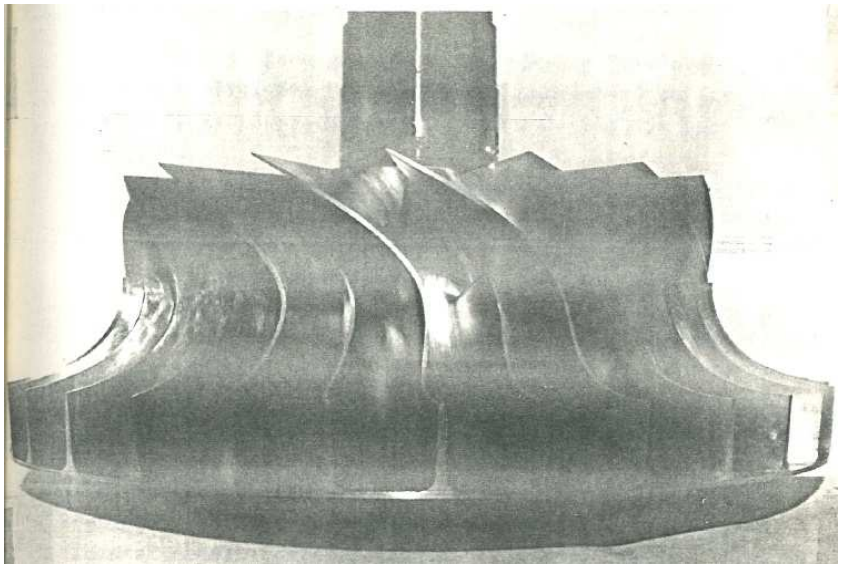

Fig. 4. *The impeller of the 410.B1baseline stage [7]*

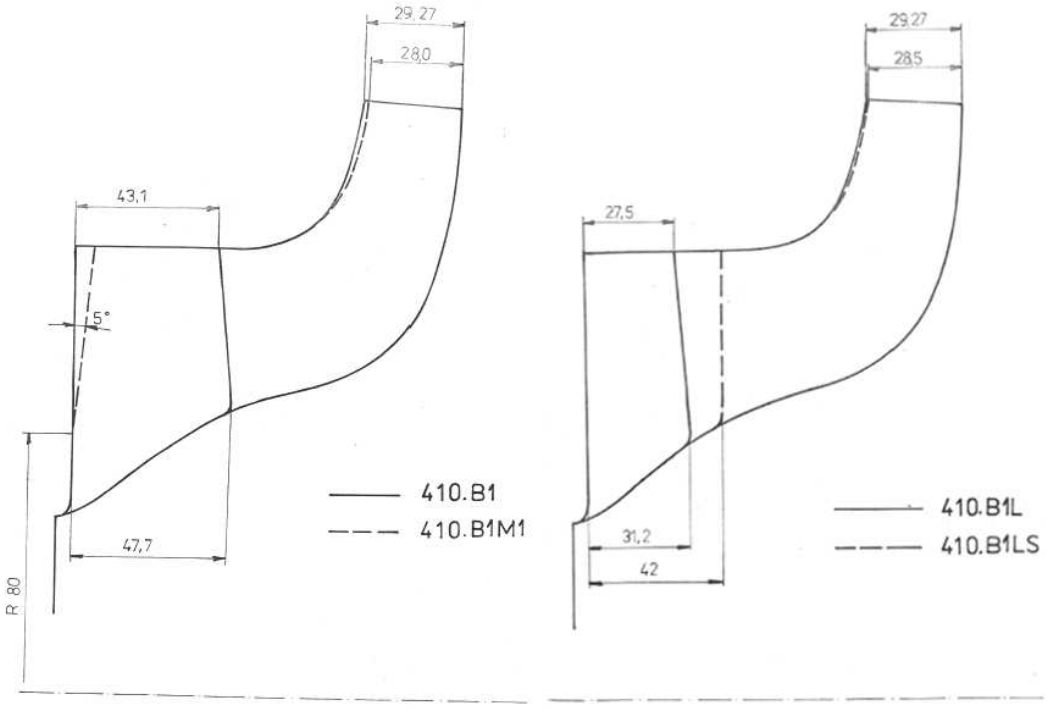

Fig. 3. *Meridional sections of various alternatives of the baseline stage [7].*

2.2 Baseline stage computational model setup

After the selection of the baseline geometry, the most suitable turbulence model had to be selected.

According to the recommendations presented in [1], the RNG *k-ε* model was the first model to be tested. The authors of [1] claim the RNG *k-ε* model provides a reasonable accuracy without investing an excessive amount of computational time. In addition to the recommendations

concerning choice of the most suitable turbulence model, the values of inlet turbulent parameters suitable for modeling flow in small-sized centrifugal compressor stages are provided in [1]. Thus, a turbulence intensity of 5% along with a turbulent length scale of 10 mm were set at the compressor inlet.

Since the flow inside a centrifugal compressor stage is always unsteady and involves both rotating and stationary reference frames, a question of modeling the interface between the impeller and diffuser is also of significant importance. A comparison of various approaches to modeling this interface can be found in [6]. In the first computations, the flow was considered to be steady, which, according to [6], can be a reasonable approximation, widely used in practice.

For steady computational models, two types of impeller-diffuser interface models are available in ANSYS CFX: the mixing plane model (named *Stage*) and the *frozen rotor* model. As described in [3], the mixing plane model is based on circumferential averaging of flow quantities at the impeller exit, assuming that the losses caused by circumferential mixing are equal to those which arise during a gradual mixing process inside the diffuser. Thus the flow disturbances which develop inside the impeller vanes do not transfer to the downstream diffuser. Although this assumption is incorrect, the mixing plane model is frequently used in turbomachinery development.

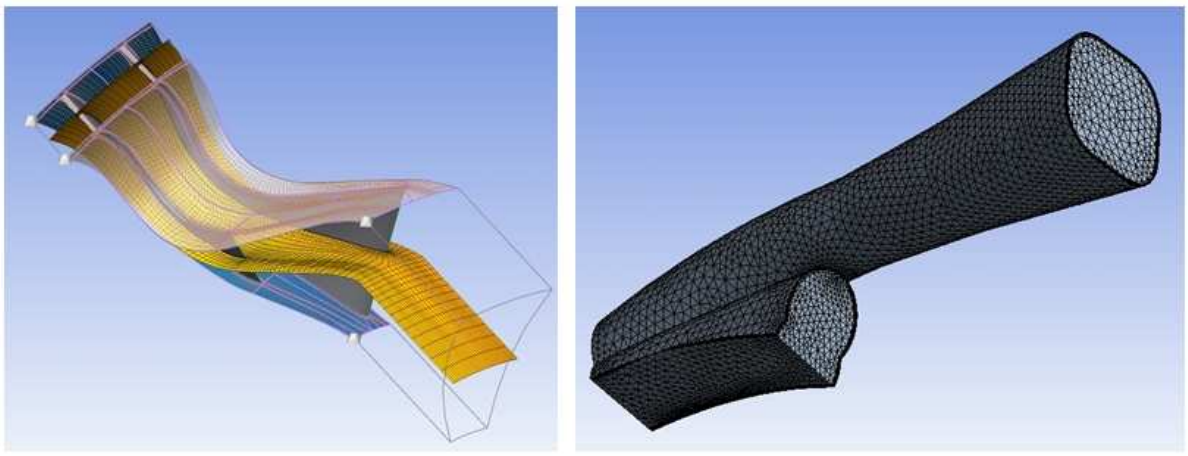

Fig. 5. *Left, the impeller computational mesh. Right, the diffuser mesh*

In opposition to the mixing plane model, the frozen rotor model does transfer flow disturbances across the impeller-diffuser interface. The drawback of this approach is that it only does so at one instance in time so the unsteady nature of the flow is not captured correctly. In [6], the two above-mentioned stationary models are compared to the unsteady *transient sliding mesh* model, the mixing plane model being more accurate that the frozen rotor. Therefore, the mixing plane model was used in our case.

As boundary conditions, a combination of total pressure and total temperature at inlet with mass flow at outlet was used.

The 3D mesh (see Fig. 5) was generated in ANSYS TurboGrid. For the reason of saving computational time during the calibration process which involves a lot of computational runs,

one impeller channel together with one diffuser channel is modeled. The impeller mesh consisted of approx. 400,000 cells in each channel while the diffuser mesh had 97,000 cells in each channel.

2.3 Baseline stage computational model results

The RNG *k-ε* model proved to describe the performance curves at various shaft speeds with a maximum error of 5.38% of the total pressure ratio (see Fig. 6). The total pressure at the outlet of the stage was underestimated in all cases. When searching for the sources of this error which was said to be too high, the values of y^+ at the diffuser walls as well as within its volume were examined (see Tab. 2) and found to exceed the values recommended by [1] in which the authors state that the value of y^+ should not be higher than 200.

Tab. 2. *Values of y^+ in the impeller and diffuser when using the first boundary layer cell thickness of 0.2 mm in the diffuser*

	Impeller	**Diffuser**
Blade / wall y^+ (area ave.)	21.1	218.3
Domain y^+ (volume ave.)	38.2	178.0

The first cell within the boundary layer had a height of 0.2 mm. Therefore, its height was reduced to 0.1 mm. By doing this, the precision of the computations increased significantly and the performance curves were now estimated very closely in terms of total pressure ratio (see Fig. 9 and Fig. 10). The isentropic efficiency was overestimated by a nearly constant value of 1.5% at nominal speed and by 2.0% at 80% nominal speed.

After these computations with the RNG *k-ε* turbulence model were made, some more turbulence models were tested, namely the common *k-ε* model, *k-ε* EARSM, *k-ω*, *k-ω* SST, BSL EARSM, and SSG Re-stress, in order to find out whether there is a more suitable model. All of these models were tested in two points along the performance curve which corresponds to the nominal shaft speed (25,000 rpm). These were the two leftmost points on the measured performance curve with a mass flow parameter of 1.356, and 1.370, respectively (see Fig. 6). The relative errors of total pressure ratio (denoted $\Delta\pi$)are given in Tab. 3. It can be seen that the RNG *k-ε* turbulence model really is the most accurate of the tested models.

Tab. 3. *Errors of total pressure ratio when using various turbulence models*

	$\Delta\pi$ at Pt. 1 (Q = 1.356)	**$\Delta\pi$ at Pt. 2 (Q = 1.370)**
RNG *k-ε*	−2.36 %	+0.36 %
k-ε	−2.91 %	−5.28 %
k-ε EARSM	+2,28 %	+2.20 %
k-ω	+8,97 %	+9.60 %
k-ω SST	+3,13 %	−4.64 %
BSL EARSM	+3,63 %	−4.33 %
SSG Re-stress	–0.37 %	−5.33 %

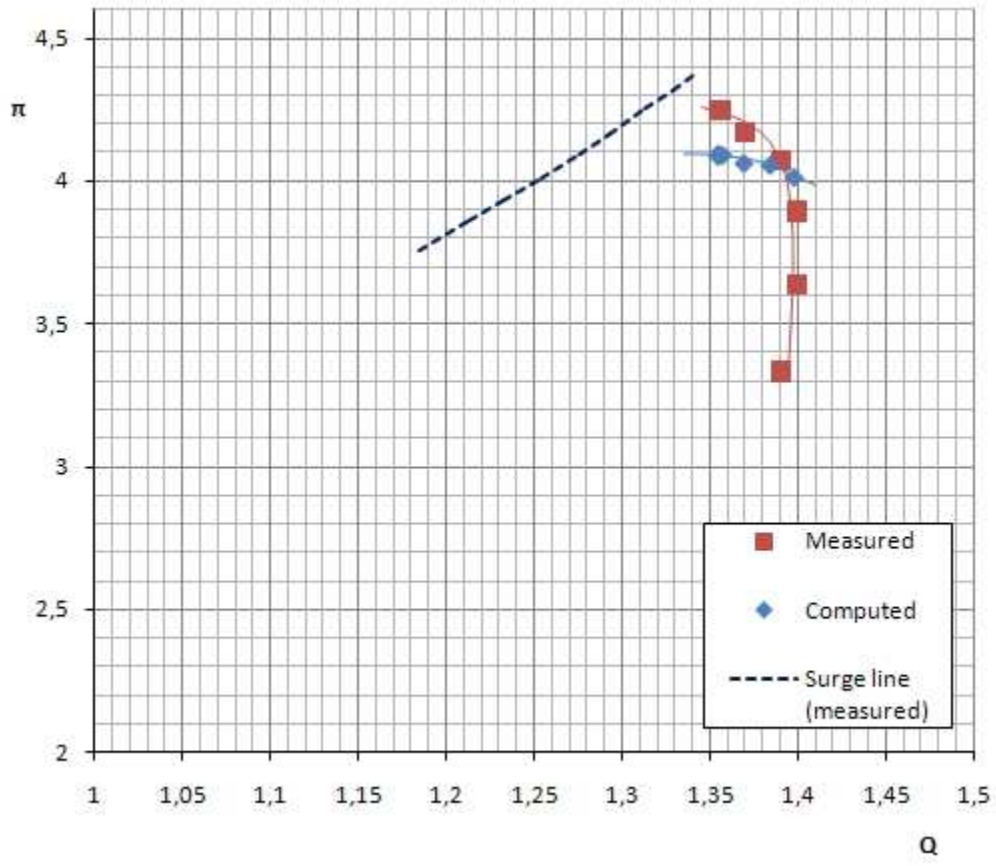

Fig. 6. *A comparison of the measured and computed performance curves (the first numerical model).*

3 Stages with a tandem-bladed impeller

Two tandem-bladed stages have been tested so far. They are denoted Stage A (with variations A1, A2, A3) and Stage B.

The impellers of all of these stages consist of an axial vane of 16 blades with circular-arc centerlines (designed using a method presented in [4]), and a radial vane of 32 splitter blades.

The axial vanes are different in Stage A and Stage B since they are designed for different total pressure ratios. Therefore, they have different curvatures. The axial vane of Stage A should have a total pressure ratio of 1.1 while the one of Stage B should achieve a value of 1.2.

The front parts of the splitter blades (one-third of their centerline downstream of the leading edge) are modified so that they have an inlet stagger angle which corresponds to the outlet angle of the axial vane, and the remaining two-thirds are kept the same as in the original stage.

Two tandem-bladed stages have been tested so far. They are denoted Stage A (with variations A1, A2, A3) and Stage B.

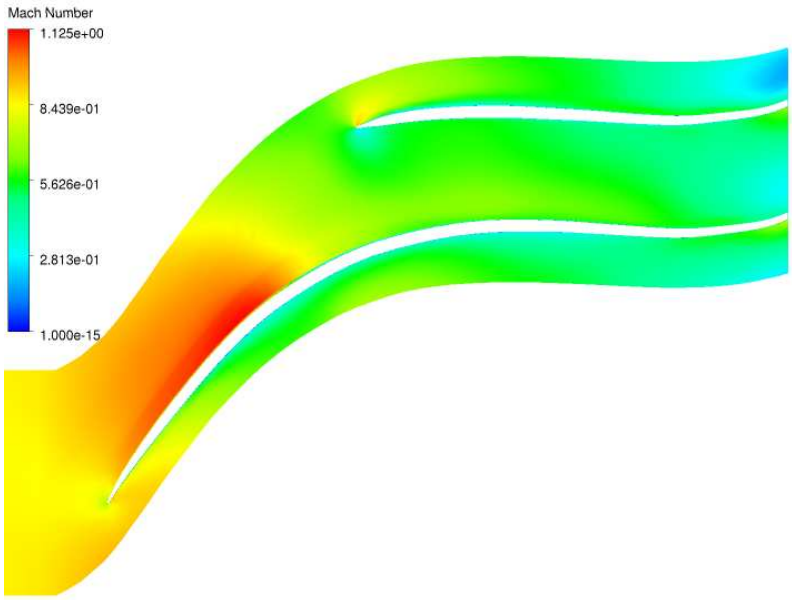

Fig. 8. *Mach number distribution inside the baseline stage impeller at 50 % span*

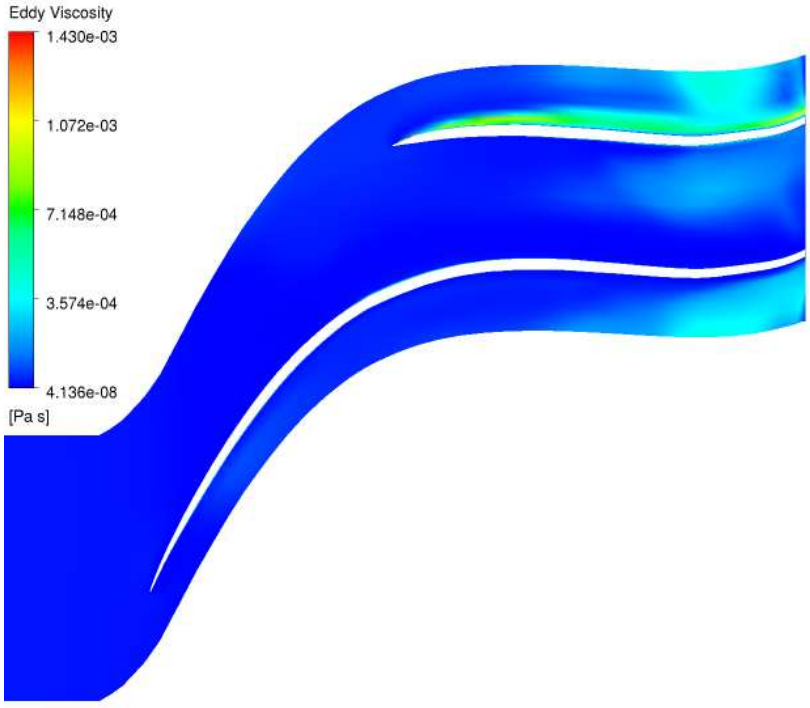

Fig. 7. *Eddy viscosity distribution inside the baseline stage impeller at 75 % span*

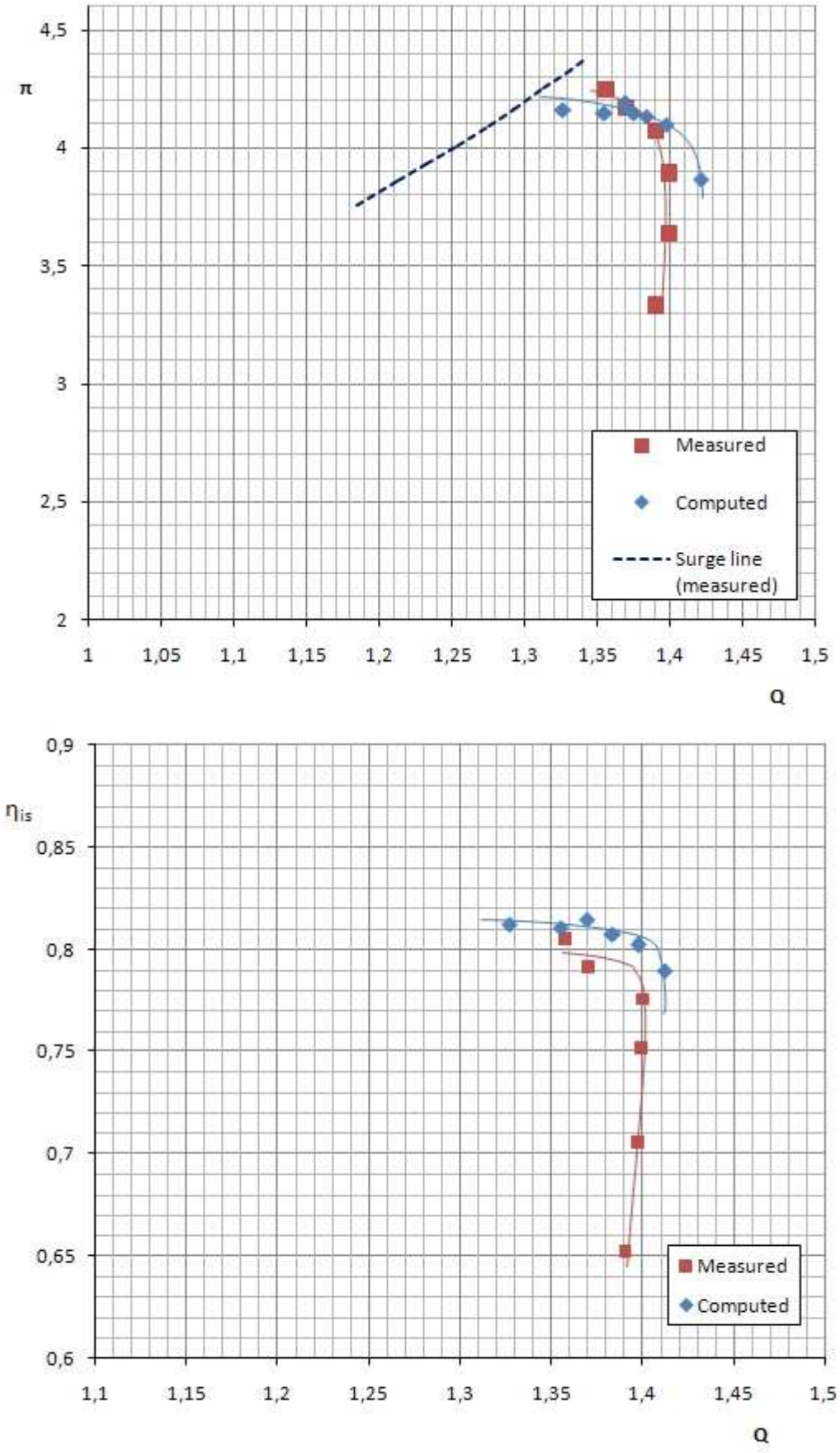

Fig. 9. *Above, a comparison of measured and computed performance curves at nominal speed. Below, a comparison of isentropic efficiencies*

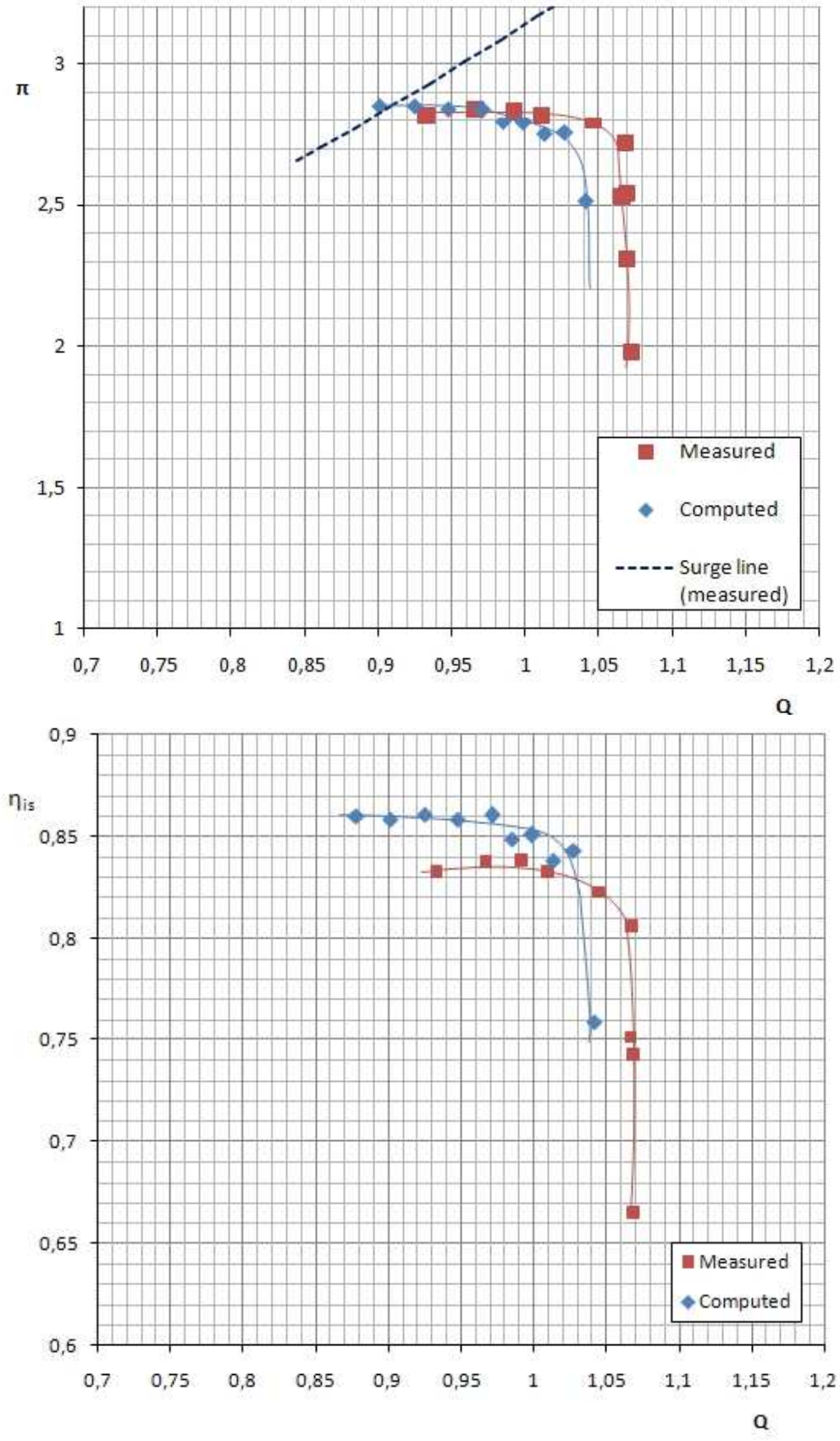

Fig. 10. *Above, a comparison of measured and computed performance curves at 80% nominal speed*
Below, a comparison of isentropic efficiencies

The circumferential position of the splitter blades, denoted by Δ_1 and Δ_2 in Fig. 11 and measured in % of the axial vane pitch, varies from stage to stage. These positions are given in Tab. 4.

The outer dimensions of the impeller, its meridional shape, and whole of the diffuser remain unchanged.

Tab. 4. *Geometry of Stages A and B*

	Stage A1	**Stage A2**	**Stage A3**	**Stage B**
Design point AoA [deg]	4			4
Blade curvature – hub [deg]	13.73			30.44
Blade curvature – tip [deg]	3.67			9.44
Splitter position – hub [% pitch]	32/82	37/87	39/89	20/70
Splitter position – tip [% pitch]	29/79	34/84	36/86	39/89

The results of the computations are presented in Fig. 14 and Fig. 15.

The results for the stages A1 to A3 show that the total pressure ratio can be increased by introducing tandem blading. This effect, however, strongly depends on the circumferential position of the splitter blades. The best results were achieved for the Stage A3 the splitter blades of which are nearest to the suction sides of the axial blades.

From this, it seems that for each tandem-bladed stage, an optimum circumferential position of the splitter blades can be found.

The stages A1 to A3, however, suffered from a low axial blade curvature which prevented them from even achieving the same values of the mass flow parameter as the baseline stage. The mass flow parameter at choke limit is about 0.07 units lower. The isentropic efficiency of these stages was, in the best case, about the same as the baseline stage had.

So, although Stage A showed the ability of correctly designed tandem-bladed stages to exceed the parameters of the conventional stages of the same size, installing it into an aeronautical engine would not bring any major benefits.

Stage B, the axial vane of which was designed to have a total pressure ratio of 1.2, has so far been tested with a single position of the splitter blades. The results of the computation are presented in Fig. 14.

Since the axial blades of this stage have a greater curvature, the mass flow parameter is the same as that of the baseline stage. The total pressure ratio is now, along whole of the performance curve, about 0.2 higher than that of the baseline stage which is a difference of about 5%. The overall size of the aeronautical engine can be reduced by using this stage.

The isentropic efficiency is, in the best case, about 1% higher than that of the baseline stage. This means that the fuel consumption of the aeronautical engine would decrease if this stage was used.

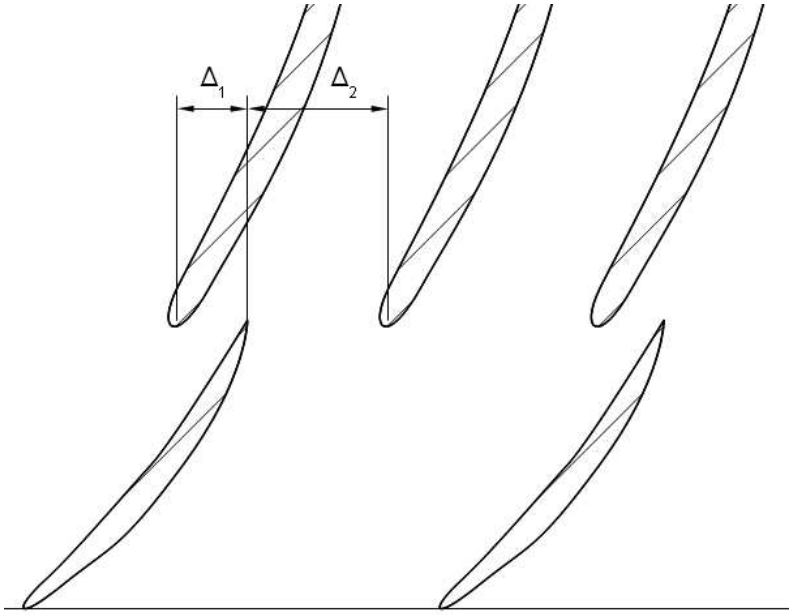

Fig. 11. *The conception of tandem impeller blading*

4 Conclusions

In this paper, recent progress in developing a tandem-bladed centrifugal compressor stage was presented.

It the first step, a computational model of the baseline stage was discussed. The search for the most suitable grid density and turbulence model was described and then the results of the optimised computation were presented. It can be stated that a model which properly describes the integral parameters of the baseline compressor stage (its total pressure ratio, isentropic efficiency, and mass flow parameter) has been found. The dependence of total pressure ratio on mass flow parameter is approximated very closely though a wider stable mass flow range is computed than it was measured. The isentropic efficiency is overestimated by a nearly constant value of approx. 1.5% at nominal speed.

After this model was found, the tandem blading was introduced into the stage. The first tandem bladed stage denoted A1 to A3, showed that the total pressure ratio can be increased by tandem blading. However, its isentropic efficiency was, in the best case, about the same as that of the baseline stage, and the mass flow parameter was lower by about 0.07. This was apparently caused by smaller throat areas inside the impeller. It was also shown that there exists an optimum position of the splitter blade leading edges against the axial vane, and that the parameters of the stage are very sensitive to this position.

The last stage to be computed so far was the stage denoted by B the axial vane of which has a greater curvature than the one which was used in stages A1 to A3. This was done in order to increase the mass flow parameter of the stage. Only one splitter blade position has been tested so far. The results obtained by the computation of stage B have shown that a greater axial vane curvature not only leads to increasing the mass flow parameter but also to a greater total

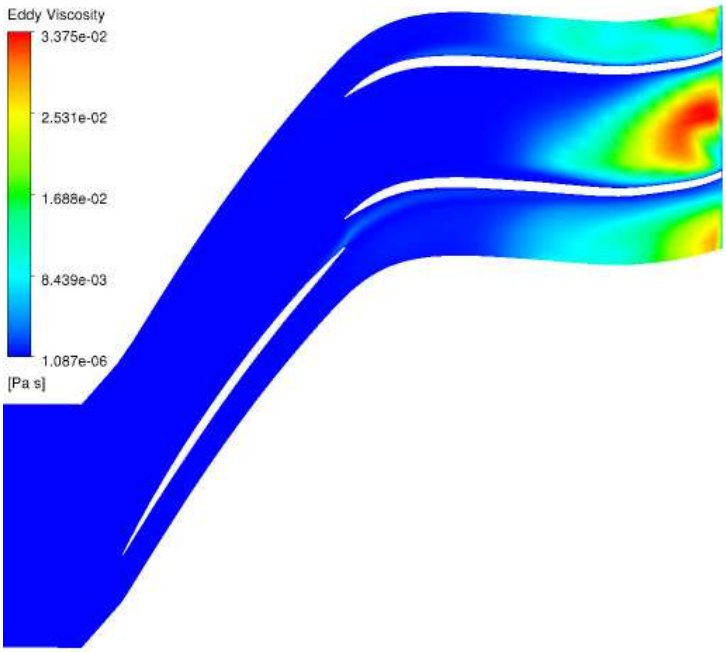

Fig. 12. *Eddy viscosity distribution inside the Stage B impeller at 75 % span*

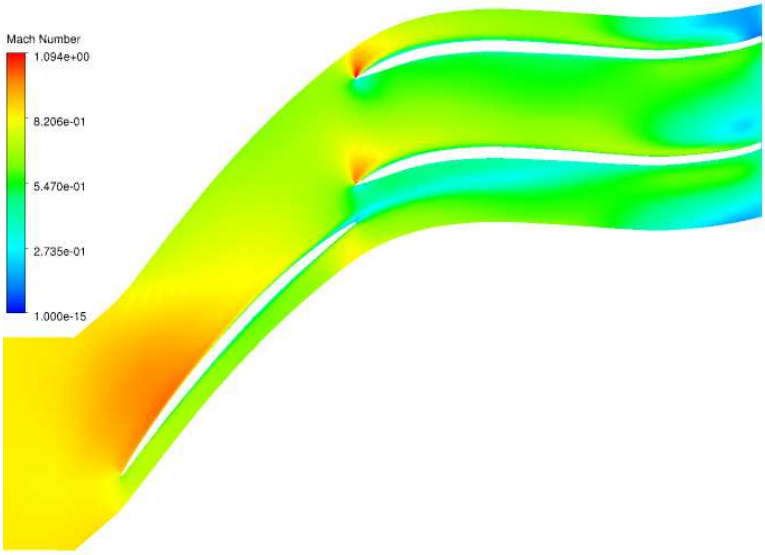

Fig. 13. *Mach number distribution inside the Stage B impeller at 50 % span*

pressure ratio, and isentropic efficiency. The mass flow range was found to be about the same as that of the baseline stage, while the total pressure ratio was increased by 0.2, and the isentropic efficiency by about 1% along most of the performance curve.

It can be said that using tandem blading really brings a possibility of increasing all the integral parameters examined while keeping the outer dimensions of the original stage unchanged. If introduced into production, this type of stage can reduce fuel consumption, emissions and weight of aeronautical engines.

List of symbols

k	Turbulent kinetic energy	$(m^2.s^{-2})$
m	Mass flow	$(kg.s^{-1})$
p	Pressure	(Pa)
Q	Mass flow parameter	$(kg.s^{-1}.K^{1/2}.Pa^{-1})$
T	Temperature	(K)
y^+	Dimensionless distance from the wall	(1)
ε	Turbulent eddy dissipation	$(m^2.s^{-3})$
η_{is}	Stage isentropic efficiency	(-)
π	Stage total pressure ratio	(-)
ω	Specific rate of turbulent kinetic energy dissipation	(s^{-1})

	Subscripts:
1	stage inlet
tot	total pressure/temperature

References

[1] AGHAEI TOG, R. – TOUSI, A. M. – TOURANI, A. *Comparison of turbulence methods in CFD analysis of compressible flows in radial turbomachines*. In: Aircraft Engineering and Aerospace Technology. Vol. 80, Iss. 6, 2008. pp. 657-665. ISSN 1748-8842.

[2] BATURIN, O.V. – KOLMAKOVA, D. A. – MATVEJEV, V. N. *Issledovanije rabočego processa centroběžnogo kompressora s pomoščju čislennych metodov gazovoj dinamiki* [*Исследование рабочего процесса центробежного компрессора с помощью численных методов газовой динамики*]. Samara: SGAU, 2013. 160 s.

[3] DENTON, John D. *Some limitations of turbomachinery CFD*. In: Proceedings of ASME Turbo Expo 2010: Power for Land, Sea and Air. Glasgow, 2010.

[4] FAROKHI, Saeed. *Aircraft Propulsion*. John Wiley & Sons, 2009.

[5] HANUS, Daniel et al. *First stage of the centrifugal compressor design with tandem rotor blades*. In: Proceedings of ISABE 2005. München, 2005.

[6] LIU, Zheji – HILL, D.L. *Issues surrounding multiple frames of reference models for turbo compressor applications*. In: International Compressor Engineering Conference, 2000.

[7] VANĚK,Václav – MATOUŠEK, Oldřich. *Situační zpráva k výzkumu a vývoji dvoustupňového dvouhřídelového odstředivého kompresoru (DDOK). II. etapa výzkumu a vývoje izolovaných stupňů.* Praha: VZLÚ, 1986.

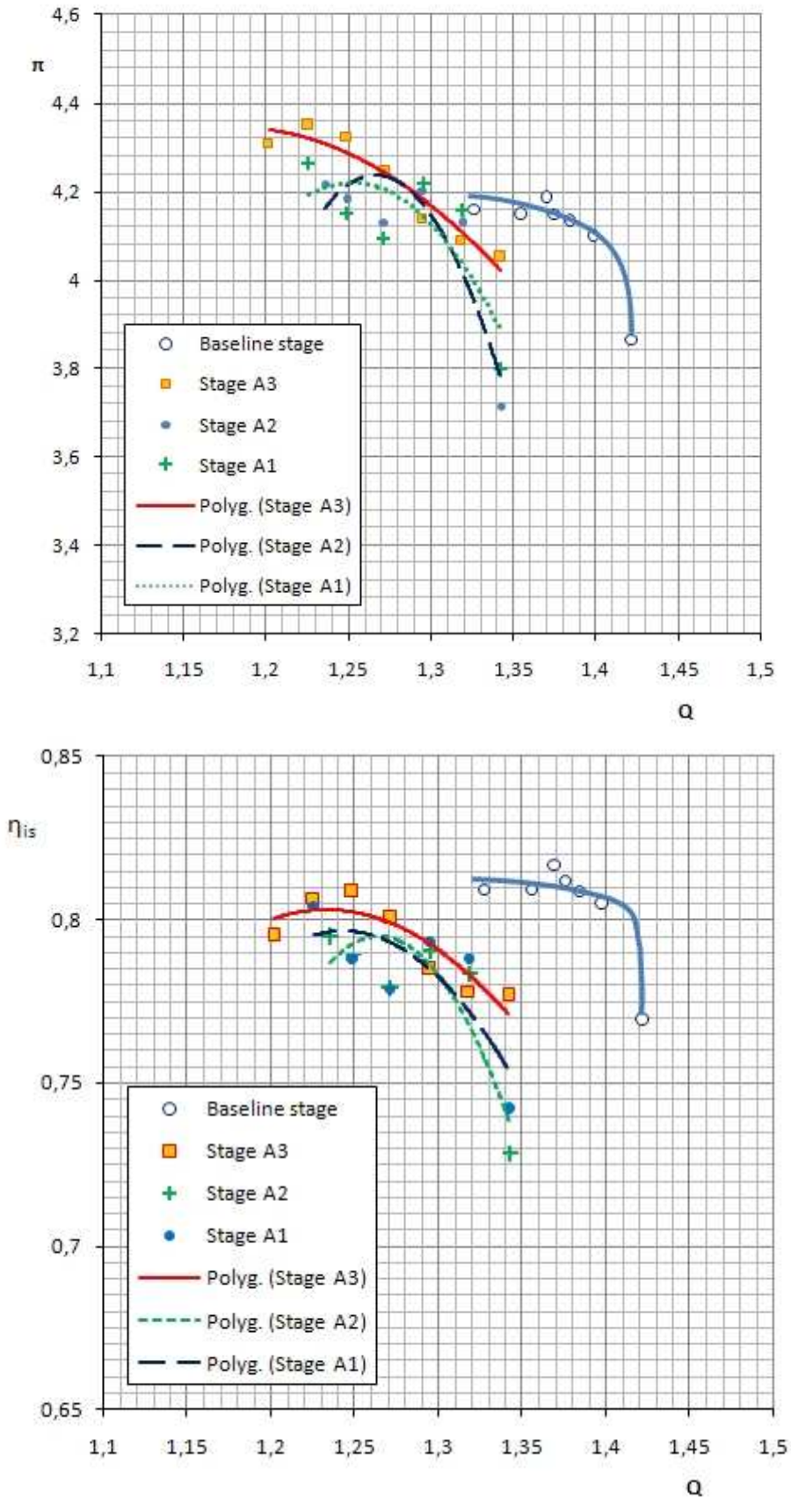

Fig. 14. *Above, a comparison of computed performance curves of the baseline and the tandem-bladed Stages A1 to A3 at nominal speed. Below, a comparison of isentropic efficiencies*

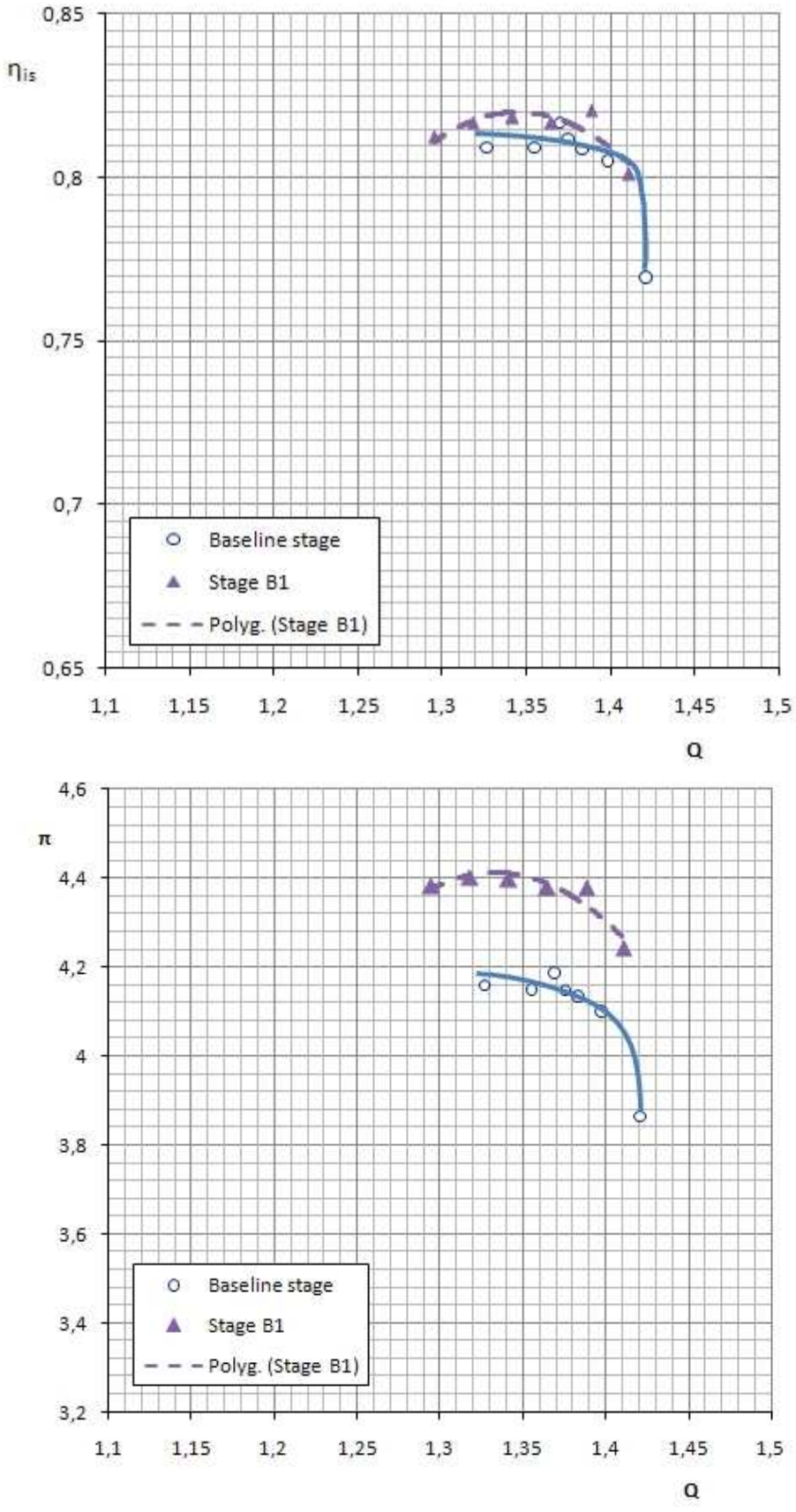

Fig. 15. *Above, a comparison of computed performance curves of the baseline and the tandem-bladed Stage B at nominal speed. Below, a comparison of isentropic efficiencies*